INTERNATIONAL JOURNAL OF SYSTEMATIC AND EVOLUTIONARY MICROBIOLOGY

RESEARCH ARTICLE

Gao *et al.*, *Int. J. Syst. Evol. Microbiol.* 2023;73:005903

DOI 10.1099/ijsem.0.005903

MICROBIOLOGY SOCIETY

Cytobacillus spongiae sp. nov. isolated from sponge *Diacarnus spinipoculum*

Luyao Gao, Qianqian Song, Jin Sang, Yilin Xiao and Zhiyong Li*

Abstract

A novel Gram-stain-positive, aerobic and motile bacterium, designated strain CY-G^T, was isolated from a sponge (*Diacarnus spinipoculum*) collected from the Red Sea. The strain grew at 13–43 °C (optimum 30 °C), pH 5.5–10.0 (optimum pH 9.0) and with 0–8.0% (w/v) (0–1.37 M) NaCl (optimum 0%). The results of phylogenetic analysis based on the 16S rRNA gene sequences indicated that CY-G^T represents a member of the genus *Cytobacillus*, with the highest sequence identity to *Cytobacillus oceanisediminis* H2^T (97.05%), followed by *Cytobacillus firmus* IAM 12464^T (96.76%). The major cellular fatty acids (>5% of the total) of CY-G^T were $C_{15:0}$iso, $C_{16:0}$iso, $C_{16:1}\omega 7c$ alcohol, $C_{16:0}$, $C_{17:1}$iso $\omega 10c$ and $C_{17:0}$iso. The major polar lipids were glycolipid, diphosphatidylglycerol, phosphatidylethanolamine and phosphatidylglycerol. The major respiratory quinone is menaquinone-7 (MK-7). The cell-wall peptidoglycan contains *meso*-diaminopimelic acid. The total genome size of CY-G^T is 4789051 bp. The DNA G+C content is 38.83 mol%. The average nucleotide identity and DNA–DNA hybridization among CY-G^T and type strains of other species of the genus *Cytobacillus* were 76.79–78.97% and 20.10–24.90%, respectively. On the basis of the results of phylogenetic analysis, physiological and biochemical characterization, strain CY-G^T represents a novel species of the genus *Cytobacillus*, for which the name *Cytobacillus spongiae* sp. nov. is proposed. The type strain is CY-G^T (=MCCC 1K06383^T=KCTC 43348^T).

At the time of writing the genus *Cytobacillus* contained 14 species with validly published names and one species with a non-validly published name, according to IJSEM Validation Lists and IJSEM articles, including *Cytobacillus firmus* (type species), *Cytobacillus ciccensis*, *Cytobacillus depressus*, *Cytobacillus eiseniae*, *Cytobacillus formosensis*, *Cytobacillus gottheilii*, *Cytobacillus horneckiae*, *Cytobacillus kochii*, *Cytobacillus luteolus*, *Cytobacillus oceanisediminis*, *Cytobacillus praedii*, *Cytobacillus purgationiresistens*, *Cytobacillus solani*, *Cytobacillus suaedae* and '*Cytobacillus stercorigallinarum*'. Species of the genus *Cytobacillus* have been isolated from plants [1, 2], soil [3–7], the intestinal tract of an earthworm [8], water [9, 10], a pharmaceutical manufacturing site [11], a spacecraft-assembly clean room [12] and food [13] (Table 1).

Sponges are sources of novel microbes [14]. In this study, a strain, designated CY-G^T, was isolated from a sponge collected from the Red Sea (29° 31′ 28.1″ N, 34° 56′ 05.5″ E) in December 2020. The sponge sample was identified on the basis of 28S rRNA and cytochrome oxidase subunit I (COI) gene sequences with 99.39 and 99.55% identity to *Diacarnus spinipoculum*, respectively. The sponge sample's 28S rRNA and COI gene sequences have been deposited into the GenBank database under the accession numbers OP895662 and OQ384973, respectively. In this study, we report the taxonomy of the novel strain CY-G^T. The results of phenotypic, chemotaxonomic, genetic and phylogenetic analyses establish the affiliation of this strain to a novel species of the genus *Cytobacillus*.

An approximately 0.2×0.2 cm section of the sponge sample was sonicated at 60 Hz for 2 min in 1 ml 1×PBS buffer solution (NaCl 136.89 mM; KCl 2.67 mM; Na2HPO4 8.1 mM; KH2PO4 1.76 mM) which is purchased from Sangon Biotech (Shanghai,

Author affiliations: [1]State Key Laboratory of Microbial Metabolism, School of Life Sciences and Biotechnology, Shanghai Jiao Tong University, Shanghai 200240, PR China.
***Correspondence:** Zhiyong Li, zyli@sjtu.edu.cn
Keywords: *Cytobacillus spongiae*; polyphasic taxonomy.
Abbreviations: AL, aminolipid; ANI, average nucleotide identity; APL, aminophospholipid; dDDH, digital DNA–DNA hybridization; DPG, diphosphatidylglycerol; GBDP, genome blast distance phylogeny method; GL, glycolipid; MK, menaquinone; PE, phosphatidylethanolamine; PG, phosphatidylglycerol; PI, phosphatidylinositol; PIM, phosphatidylinositol mannoside; PL, unidentified phospholipid.
The GenBank accession numbers for the 16S rRNA gene sequence and the whole-genome sequence of CY-G^T are OP869988.1 and CP089997, respectively.
Six supplementary figures and one supplementary table are available with the online version of this article.

Table 1. Differential characteristics of CY-G^T and the members of the genus *Cytobacillus*

Strains: 1, *Cytobacillus spongiae* CY-G^T; 2, *Cytobacillus oceanisediminis* H2^T; 3, *Cytobacillus firmus* IAM 12464^T; 4, *Cytobacillus depressus* BZ1^T (data from [4]); 5, *Cytobacillus gottheilii* WCC 4585^T (data from [11]); 6, *Cytobacillus ciccensis* 5L6^T (data from [1]); 7, *Cytobacillus suaedae* HD4P25^T (data from [2]); 8, *Cytobacillus solani* FJAT 18043^T (data from [5]); 9, *Cytobacillus formosensis* CC-LY275^T (data from [9]); 10, *Cytobacillus kochii* WCC 4582^T (data from [13]); 11, *Cytobacillus horneckiae* 1P01SC^T (data from [12]); 12, *Cytobacillus praedii* FJAT 25547^T (data from [6]); 13, *Cytobacillus luteolus* YIM 93174^T (data from [7]); 14, *Cytobacillus eiseniae* A1-2^T (data from [8]); 15, *Cytobacillus purgationiresistans* DS22^T (data from [10]). +, Positive; w, weakly positive; –, negative, ND, no data available; AL, aminolipid; APL, aminophospholipid; DPG, diphosphatidylglycerol; GL, glycolipid; PE, phosphatidylethanolamine; PG, phosphatidylglycerol; PI,phosphatidylinositol; PIM, phosphatidylinositol mannoside; PL, phospholipid.

Characteristic	1	2	3	4	5	6	7	8	9	10	11	12	13	14	15
Isolated from	Sponge (*Diacarnus spinipoculum*)	Marine sediment	Garden soil	Sunflower field soil	Pharmaceutical production line	Seeds of hybrid maize (*Zea mays* L., Jingke 968)	Halophyte *Suaeda salsa*	Rhizosphere soil of a potato field	Pesticide wastewater	Dairy food	Clean room of the Kennedy Space Center	Purplish paddy soil	Salt field	Intestinal tract of earthworm (*Eisenia fetida* L.)	Water of drinking-water treatment plant
Growth conditions															
Temperature range (°C)	13–43	4–45	10–40	6–40	10–40	4–45	10–40	20–45	20–45	10–40	4–50	15–40	15–45	15–37	15–37
Optimum	30	37	37	30–33	30	30	30	35	30	30	30	30	28–37	30	30
pH range	5.5–10.0	6.0–10.0	5.5–9.0	6.0–9.0	7.0–9.5	6.0–11.0	7.0–9.5	6.0–10.0	7.0–8.0	6.0–10.5	ND	5.0–12.0	6.0–8.0	6.5–11.0	7.0–10.0
Optimum	9.0	7.0	6.0	7.0	8.0	7.0	7.5	9.0	8.0	7.0	7.0	9.0	7.0	7.0	7.0–8.0
NaCl range (%)	0–8.0	0–13.0	0–14.0	0–5.5	0–8.5	0–9.0	0–5.0	0–10.0	0–6.0	0–10.0	0–10.0	0–10.0	0–10.0	0–9.0	0–8.0
Optimum	0	ND	2.0	0.5	0.5	0	1.0	0	0	0.5	ND	4.0	0–2.0	ND	1.0–3.0
Genome															
DNA G+C content (mol %)	38.8	44.8	43.7	44.5	38.7	37.4	36.4	48.8	37.9	36.4	35.6	39.1	36.9	38.5	36.5
ANI (%)	CY-G^T *vs.*	77.52	78.97	77.77	ND	ND	78.78	78.73	ND	ND	78.00	77.21	76.79	77.66	ND
Alignment fraction (AF)		0	0	0	ND	ND	0.15	0	ND	ND	0	0.06	0	0.09	ND
DDH (%)		20.10	22.70	22.00	ND	ND	24.90	23.30	ND	ND	24.00	22.00	20.20	22.50	ND
16S rRNA gene sequence identity (%)		97.05	96.76	96.64	96.62	96.3	96.14	96.45	95.89	96.36	96.74	96.27	94.95	95.64	96.13
Enzymatic activity:															
Oxidase (EC 1.1.3.13)	w	w	w	+	–	–	+	+	+	–	–	–	–	–	+
Catalase (EC 1.11.1.6)	+	+	+	+	+	+	+	+	+	+	+	+	+	+	+
Urease (EC 3.5.1.5)	–	–	–	+	ND	–	+	–	+	ND	–	–	+	–	–
Alkaline phosphatase (EC 3.1.3.1)	+	+	w	+	w	ND	–	ND	+	+	w	+	+	–	–
Valine arylamidase (EC 3.4.11.2)	w	–	w	w	–	ND	–	ND	ND	w	–	–	–	–	+
Trypsin (EC 3.4.21.4)	w	w	w	–	–	ND	+	ND	+	w	–	–	–	–	–
Acid phosphatase (EC 3.1.3.2)	+	w	w	+	–	ND	–	ND	+	w	–	–	–	–	–
β-Glucuronidase (EC 3.2.1.31)	w	–	–	–	–	ND	–	ND	–	–	–	–	–	–	–

Continued

Table 1. Continued

Characteristic	1	2	3	4	5	6	7	8	9	10	11	12	13	14	15
α-Glucosidase (EC 3.2.1.20)	+	+	+	–	W	ND	+	ND	–	–	–	+	+	–	–
β-Glucosidase (EC3.2.1.21)	W	–	–	–	W	ND	–	ND	–	–	–	–	–	–	–
α-Mannosidase (EC 3.2.1.24)	–	+	–	–	–	ND	–	ND	–	–	–	–	–	–	–
Acid production from:															
Glycerol	–	–	W	ND	W	+	ND	–	ND	W	–	+	W	–	–
(–)-Ribose	–	–	–	+	–	+	ND	–	ND	W	–	+	–	–	–
(+)-Xylose	–	–	–	+	–	–	ND	–	ND	–	–	–	+	+	–
(+)-Glucose	+	+	W	+	+	–	ND	–	ND	–	–	+	–	–	–
(–)-Fructose	+	+	–	W	+	–	ND	–	ND	–	–	–	+	+	–
(–)-Sorbose	–	–	–	+	–	–	ND	–	ND	–	–	–	–	–	–
(–)-Mannitol	–	–	W	–	+	+	ND	–	ND	–	–	–	–	+	–
N-Acetylglucosamine	–	W	W	ND	+	+	ND	+	ND	–	–	+	–	–	–
Arbutin	–	–	–	+	–	–	ND	–	ND	–	–	–	–	–	–
(+)-Maltose	+	+	W	–	+	+	ND	–	ND	–	–	–	–	+	–
Sucrose	–	+	+	–	+	+	ND	–	ND	–	–	–	+	–	–
(+)-Trehalose	+	+	W	–	+	–	ND	–	ND	–	–	–	–	–	–
Inulin	–	W	–	+	–	–	ND	–	ND	–	–	–	–	–	–
(+)-Raffinose	–	W	–	–	W	–	ND	–	ND	–	–	–	–	–	–
Starch	–	W	W	–	ND	–	ND	–	ND	–	–	–	+	–	–
Glycogen	–	W	–	ND	+	–	ND	–	ND	–	–	–	W	–	–
Assimilation of:															
(–)-Mannitol	–	–	+	ND	ND	–	–	ND	ND	ND	–	ND	ND	–	–
N-Acetylglucosamine	–	+	+	ND	ND	W	–	ND	–	ND	–	ND	ND	–	–
Gluconate	–	+	–	ND	ND	–	+	ND	–	ND	+	ND	ND	–	–
Malic acid	–	+	–	ND	ND	–	+	ND	W	ND	+	ND	ND	–	ND
Citrate	–	+	+	ND	ND	ND	–	ND	W	ND	+	ND	ND	–	ND
Other Reactions															
Potassium nitrate reduction	+	+	+	+	+	+	+	+	–	–	+	+	–	–	–
(+)-Glucose fermentation	+	–	–	+	ND	+	–	ND	ND	–	–	–	ND	–	–

Continued

Table 1. Continued

Characteristic	1	2	3	4	5	6	7	8	9	10	11	12	13	14	15
Aesculin hydrolysis	–	–	–	+	+	+	+	ND	ND	–	–	–	–	+	–
Gelatin hydrolysis	W	+	+	+	+	+	–	+	W	+	+	+	–	–	+
Fatty acids	$C_{15:0}$iso, $C_{16:0}$iso, $C_{16:1}$ω7c alcohol, $C_{16:0}$, $C_{17:1}$iso ω10c, $C_{17:0}$iso	$C_{15:0}$iso, $C_{15:0}$anteiso, $C_{16:0}$iso, $C_{16:1}$ ω7c alcohol, $C_{16:0}$, $C_{14:0}$iso	$C_{15:0}$iso, $C_{16:0}$iso, $C_{16:1}$ω7c alcohol, $C_{15:0}$anteiso, $C_{14:0}$iso, $C_{16:1}$iso H	$C_{15:0}$iso, $C_{15:0}$anteiso, $C_{14:0}$iso	$C_{15:0}$iso, $C_{15:0}$anteiso, $C_{17:0}$anteiso	$C_{15:0}$iso, $C_{15:0}$anteiso, $C_{16:0}$iso, $C_{14:0}$iso, $C_{17:0}$anteiso, $C_{16:1}$ω7c alcohol	$C_{15:0}$iso, $C_{15:0}$anteiso, $C_{14:1}$iso E	$C_{15:0}$anteiso, $C_{15:0}$iso, $C_{16:0}$iso, $C_{17:0}$anteiso, $C_{16:0}$, $C_{14:0}$iso	$C_{14:0}$iso, $C_{15:0}$iso, $C_{15:0}$anteiso	$C_{15:0}$iso, $C_{15:0}$anteiso, $C_{14:0}$iso, $C_{16:0}$iso	$C_{15:0}$iso, $C_{15:0}$anteiso	$C_{15:0}$iso, $C_{15:0}$anteiso, $C_{16:0}$iso, $C_{14:0}$iso	$C_{15:0}$iso, $C_{15:0}$anteiso, $C_{16:0}$iso	$C_{15:0}$iso, $C_{15:0}$anteiso, $C_{14:0}$iso	$C_{16:1}$ω7c alcohol, $C_{14:0}$iso, $C_{15:0}$iso, $C_{16:0}$iso, $C_{15:0}$anteiso
Polar lipids	DPG, PE, PG, GL	DPG, PG, PE, APL	ND	DPG, PG, PE	DPG, PG, PE, APL	DPG, PG, PE	DPG, PG, PE	DPG, PG, PE	DPG, PG, PE	DPG, PG, PE, APL	DPG, PE, PG, APL, 2AL, 7PL	DPG, PG, PE	DPG, PG, PE, PI, PIM, 2PL	DPG, PE	DPG, PG, PE

China), and then tenfold serial dilutions to the dilution of 10^{-6} with 1×PBS buffer solution were carried out. Samples (100 µl) were taken and then spread on ZoBell marine agar plates (AC12065; ACMEC). After incubation at 28 °C for 20 days, individual colonies were picked and purified by streaking for isolation. Upon identification of all isolates using 16S rRNA gene sequence, a novel member of the genus *Cytobacillus*, strain CY-G^T, was identified and maintained on lysogeny broth medium (LB) solidified with 1.5% w/v agar at 4 °C and stored in 20% (v/v) glycerol suspensions at −80 °C.

DNA was extracted using a TIANamp Bacteria DNA kit (TIANGEN) according to the manufacturer's instructions. The whole genome of CY-G^T was sequenced using a NovaSeq 6000 PE150 (Illumina) and PromethION 48 apparatus (Oxford Nanopore) at Guangdong Magigene Biotechnology (Shenzhen, Guangdong, China). After quality control, reads were assembled using SMRT Link version 5.0.1 [15], and the N50 (defined as the length of the shortest contig at 50% of the total assembly length) was 4099173 bp. The results of CheckM analysis indicated that the completeness of the CY-G^T genome was 98.72%. The genomic sequence of the strain has been uploaded to the NCBI GenBank with the accession number CP089997. The 16S rRNA gene was extracted from the whole genome sequence using RNAmmer [16], and the predicted sequence has also been uploaded to the NCBI GenBank with the accession number OP869988.1. Comparison was carried out using MUSCLE with default settings by EBI (https://www.ebi.ac.uk/Tools/msa/muscle/) to calculate percentage identities of 16S rRNA gene sequences with other type strains. As a result, strain CY-G^T was found to be closely related to *Cytobacillus oceanisediminis* H2^T (97.05%), followed by *Cytobacillus firmus* IAM 12464^T (96.76%), *Cytobacillus horneckiae* 1P01SC^T (96.74%), *Cytobacillus depressus* BZ1^T(96.64%), *Cytobacillus gottheilii* WCC 4585^T (96.62%), *Cytobacillus solani* FJAT 18043^T (96.45%), *Cytobacillus kochii* WCC 4582^T (96.36%), *Cytobacillus ciccensis* 5L6^T (96.30%), *Cytobacillus praedii* FJAT 25547^T (96.27%), *Cytobacillus suaedae* HD4P25^T (96.14%), *Cytobacillus purgationiresistans* DS22^T (96.13%), *Cytobacillus formosensis* CC-LY275^T (95.89%), *Cytobacillus eiseniae* A1-2^T (95.64%) and *Cytobacillus luteolus* YIM 93174^T (94.95%). All the sequence identities were above the value of 94.5% for genus circumscription [17], indicating that CY-G^T potentially represents a novel bacterial species of the genus *Cytobacillus*. Phylogenetic trees were reconstructed from a multiple sequence alignment using MUSCLE (gap open=−400.00; gap extent=0.00; max memory in MB=2048; max iterations=16; cluster method is UPGMA; min diag length=24) with the neighbour-joining [18], maximum-likelihood [19] and minimum-evolution [20] methods implemented with MEGA-11 [21]. Bootstrap values were calculated from 1000 replications. In the maximum-likelihood (ML) tree, CY-G^T is closely grouped with *Cytobacillus oceanisediminis* H2^T and *Cytobacillus firmus* IAM 12464^T (Fig. 1). *Cytobacillus oceanisediminis* H2^T was obtained from the Marine Culture Collection of China (MCCC) and *Cytobacillus firmus* IAM 12464^T was obtained from the China Centre for Type Culture Collection (CCTCC). These results, together with the phylogenetic trees reconstructed using neighbour-joining (NJ) and minimum-evolution (ME) methods (Figs S1 and S2 available in the online supplementary material), indicate that CY-G^T is included in the clusters of species of the genus *Cytobacillus*.

The genome size of CY-G^T was estimated to be 4789051 bp, including one chromosome and one plasmid. The total DNA G+C content was calculated from the genome with 282.0×fold coverage. The value for CY-G^T was 38.83 mol%, which lies within the range of values reported for members of the genus *Cytobacillus* (Table 1). The value is below the 10 mol% threshold cut-off for recognition of species [17]. The single-copy orthologous cluster protein sequences were extracted using Proteinortho version 6. After multi-sequence alignment of amino acid sequences using the MUSCLE programme with default settings, the maximum-likelihood phylogenetic tree was reconstructed using MEGA version 11 (Fig. 2). It indicates that *Cytobacillus spongiae* CY-G^T is a member of genus *Cytobacillus*. The average nucleotide identity (ANI) value was calculated using FastANI V.1.1 [22]. The alignment fraction (AF) value was calculated using JGI MiSI [23]. The ANI values between CY-G^T and other type strains of species of the genus *Cytobacillus* are 76.79–78.97%, which are below the 95% threshold cut-off for recognition of prokaryotic species [22]. The AF values between CY-G^T and other species of the genus *Cytobacillus* are 0–0.15, which are far below the value of 0.6 [23]. DNA–DNA hybridization (DDH) was performed using the Genome-to-Genome Distance Calculator 2.1 web service with Formula 2 (https://ggdc.dsmz.de/ggdc.php) [24]. CY-G^T showed DNA–DNA relatedness of 20.10–24.90% with type strains of other species of the genus *Cytobacillus*, which is also below the value of 70% for species circumscription [25], indicating that CY-G^T should be considered as representing a novel species of the genus *Cytobacillus*. The detailed values of ANI, AF and DDH are shown in Table 1. Genome annotation was carried out using the NCBI Prokaryotic Genome Annotation Pipeline. The results indicated that there are 4666 CDSs, 4606 genes, 147 putative rRNA genes, 11 putative 5S (*rrf*) rRNA genes, 11 putative 16S (*rrs*) rRNA genes, 11 putative 23S (*rrl*) rRNA genes, 108 putative tRNA genes, 6 putative ncRNA genes and 60 putative pseudogenes. Secondary metabolite biosynthetic gene clusters were predicted using antiSMASH 6.0 [26], terpene and T3PKS gene clusters were found in the genome of CY-G^T, which are common in the genomes of other members of the genus *Cytobacillus* (Table S1).

Cells were observed using scanning electron microscopy (SEM, Sirion 200, FEI) after incubation in LB medium at 28 °C for 2 days. Colony morphology was examined after 3 days of incubation on LB agar plates at 28 °C CY-G^T was cultured over a 10–46 °C temperature range (at intervals of 3 °C) and a 5.5–10.5 pH range (at intervals of 0.5 pH units) in LB medium. Growth at various NaCl concentrations was tested over the range of 0–16.0% (w/v) NaCl (at intervals of 1%, added externally) with incubation at 28 °C and pH 7.0 in LB medium. Anaerobic growth was determined using the AnaeroPack-Anaero (MGC) according to the manufacturer's instructions. The Gram reaction was performed using a Gram-staining kit (Solarbio).

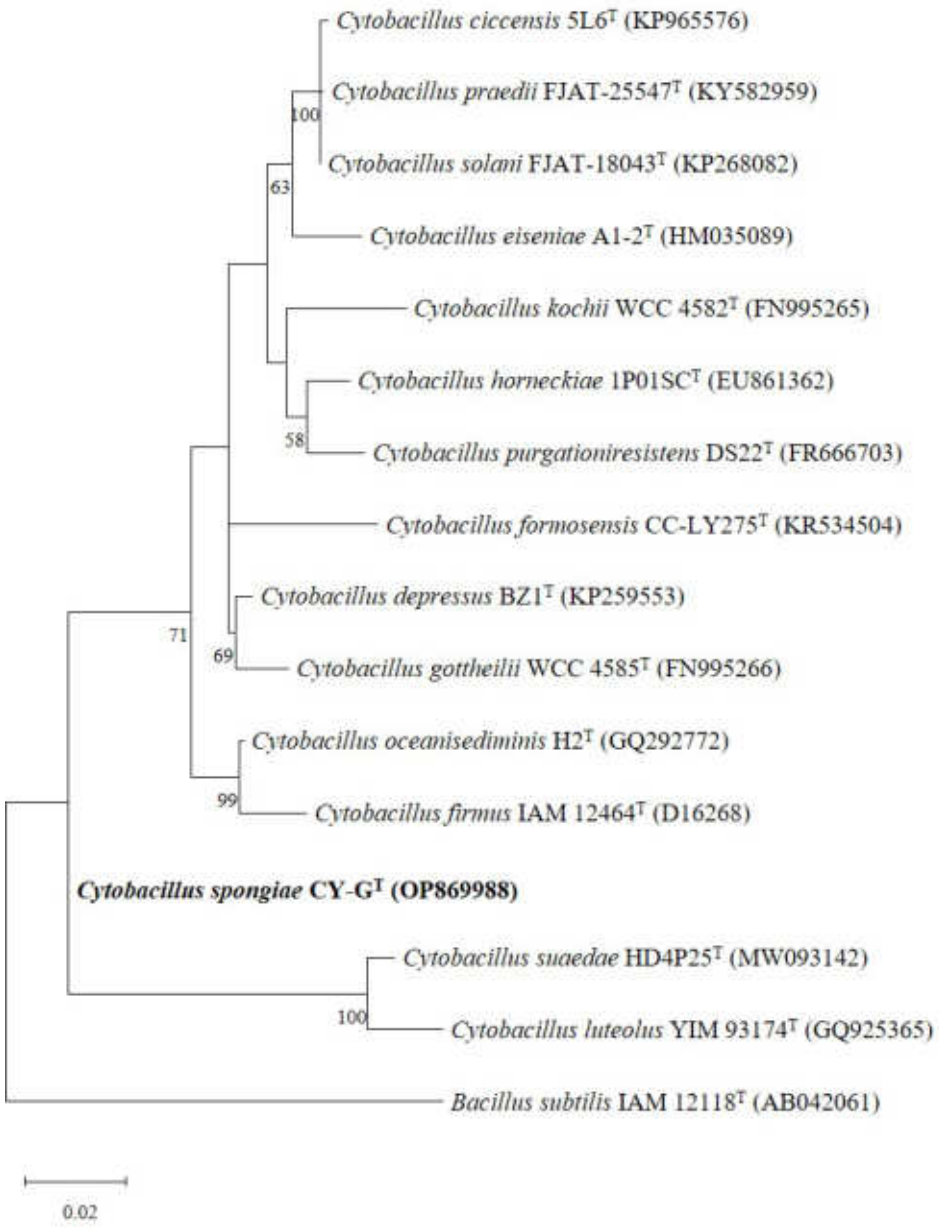

Fig. 1. Maximum-likelihood phylogenetic tree based on 16S rRNA gene sequences, showing the relationship of CY-G^T and other related type strains of species in the genus *Cytobacillus* using the general time reversible model. The tree with the highest log likelihood (−3321.42) is shown. Bootstrap values based on 1000 resampled datasets are shown at branch nodes. Initial tree(s) for the heuristic search were obtained automatically by applying Neighbor-Join and BioNJ algorithms to a matrix of pairwise distances estimated using the maximum composite likelihood (MCL) approach and then selecting the topology with the superior log likelihood value. A discrete Gamma distribution was used to model evolutionary rate differences among sites [five categories (+*G*, parameter=0.1000)]. The rate variation model allowed for some sites to be evolutionarily invariable ([+*I*], 45.08% sites). The gaps/missing data treatment was used for all sites. The branch swap filter was very strong. Bar, 0.02 substitutions per nucleotide position. This analysis involved 16 nucleotide sequences. GenBank accession numbers are included in parentheses. There were a total of 1305 positions in the final dataset. The sequence of *Bacillus subtilis* IAM 12118^T served as an outgroup.

Motility was examined on motility agar [27]. The presence of oxidase and catalase were demonstrated by the oxidation of 1% (w/v) *N*, *N*, *N*′, *N*′-tetramethyl-1,4-phenylenediamine and by bubble production in 10% (v/v) aqueous hydrogen peroxide solution, respectively.

The fatty acids were analysed by gas chromatography (model 6850; Agilent Technologies) and identified using the TSBA6.0 database of the Microbial Identification System [28]. Isoprenoid quinones were determined according to the method of Collins [29]. Polar lipids were extracted and separated on silica gel 60 aluminium-backed thin-layer plates according to the

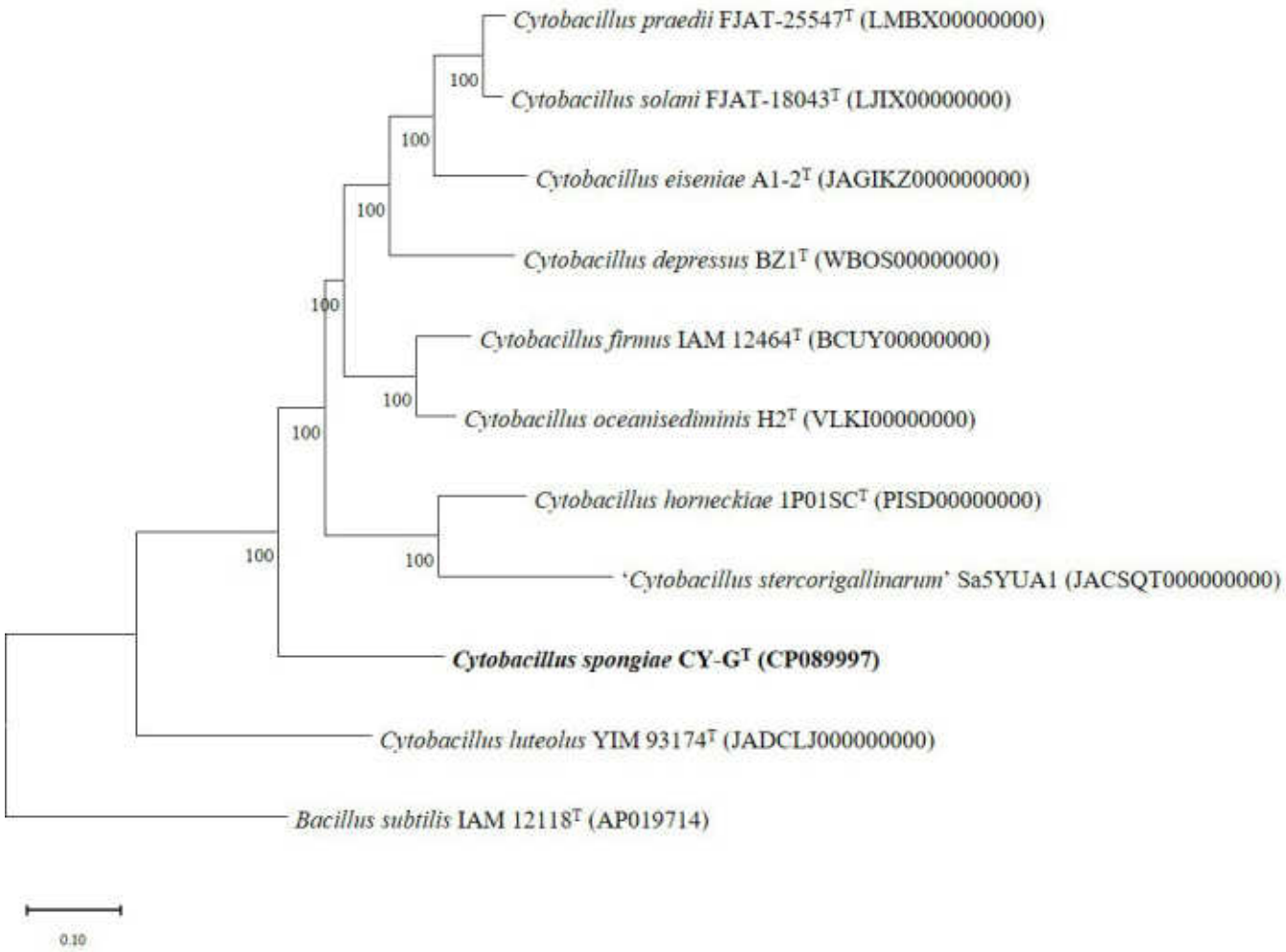

Fig. 2. Maximum-likelihood phylogenetic tree based on genome sequences, showing the relationship of CY-G^T and other related type strains of species of the genus *Cytobacillus* using the Le Gascuel 2008 model. The tree with the highest log likelihood (−2701917.23) is shown. Bootstrap values based on 250 resampled datasets are shown at branch nodes. Initial tree(s) for the heuristic search were obtained automatically by applying Neighbor-Join and BioNJ algorithms to a matrix of pairwise distances estimated using the Jones–Taylor–Thornton (JTT) model and then selecting the topology with the superior log likelihood value. A discrete Gamma distribution was used to model evolutionary rate differences among sites [five categories (+*G*, parameter=0.4266)]. The rate variation model allowed for some sites to be evolutionarily invariable ([+*I*], 25.59% sites). The gaps/missing data treatment was used for all sites. The branch swap filter was very strong. Bar, 0.10 substitutions per nucleotide position. This analysis involved 11 amino acid sequences. GenBank accession numbers are included in parentheses. There were a total of 290211 positions in the final dataset. The sequence of *Bacillus subtilis* IAM 12118^T serves as an outgroup.

method of Minnikin *et al*. [30]. Ninhydrin, α-naphthol and molybdatophosphoric acid were used to detect other polar lipids according to the method of Tindall [31]. The amino acids of the cell wall were determined as described previously [32]. API 50CH, API ZYM (bioMérieux), Biolog GNIII MicroPlate (Biolog) and API 20NE (bioMérieux) kits were used according to the manufacturers' instructions to further determine the physiological and biochemical characteristics of CY-G^T including acid production, enzyme activities, carbon source utilization and other biochemical characteristics, respectively. Resistance to antibiotics was examined by the agar diffusion technique, using commercial antibiotic discs [33] on LB agar medium and incubation at 28 °C for up to 7 days.

CY-G^T formed yellowish, round and smooth colonies and exhibited swarming after growth on LB agar plates at 28 °C for 3 days. Cells were Gram-stain-positive, like those of almost all species of the genus *Cytobacillus*, 0.7 µm in width and 3.0 µm in length and contained subterminal endospores in slightly swollen sporangia (Fig. S3). Growth was observed at 13–43 °C, pH 5.5–10.0 and with 0–8.0% (w/v) (0–1.37 M) NaCl. Optimum growth was observed at 30 °C, pH 9.0 and with 0% (w/v) NaCl (Fig. S4). The detailed physiological and biochemical characteristics of CY-G^T in comparison with other species of the

genus *Cytobacillus*. are presented in Table 1, which shows many differences between CY-G^T and other strains. For example, CY-G^T is weakly positive for the activity of β-glucuronidase but other strains are negative.

The predominant respiratory quinone in CY-G^T was identified as menaquinone-7 (MK-7), which is in agreement with the description of the genus *Cytobacillus* (Table 1). The polar lipids detected include glycolipid, diphosphatidylglycerol, phosphatidylethanolamine and phosphatidylglycerol (Fig. S5). The polar lipids of CY-G^T are different from those of other strains of species of the genus *Cytobacillus* (Table 1). The major fatty acids are $C_{15:0}$iso, $C_{16:0}$iso, $C_{16:1}$ω7*c* alcohol, $C_{16:0}$, $C_{17:1}$iso ω10*c* and $C_{17:0}$iso (Table 1), which are also distinct from those of other species of the genus *Cytobacillus*. Marginal quantitative differences were observed in the profile of fatty acids compared with other species of the genus *Cytobacillus* (Table 1). The primary cell-wall amino acids were glycine and ornithine, the diagnostic cell-wall diamino acid was *meso*-DAP (Fig. S6).

The phenotypic and chemotaxonomic properties of CY-G^T and its 16S rRNA gene sequence, along with ANI, AF and DDH values, distinguish it from other strains of species in the genus *Cytobacillus*. On the basis of the results of the present polyphasic analysis, strain CY-G^T is considered to represent a novel species within the genus of *Cytobacillus*, for which the name *Cytobacillus spongiae* sp. nov. is proposed.

DESCRIPTION OF *CYTOBACILLUS SPONGIAE* SP. NOV

Cytobacillus spongiae (spon'gi.ae. L. gen. n. *spongiae*, of a sponge, the source of the type strain)

Cells are 0.7 µm in width and 3.0 µm in length, rod-shaped, Gram-stain-positive, aerobic and motile. Cells can grow well on LB, TSB and ZoBell marine media but not on Reasoner's 2A agar medium (yeast extract 0.5 g l^{-1}; peptone 0.5 g l^{-1}; casein hydrolysate 0.5 g l^{-1}; glucose 0.5 g l^{-1}; soluble starch 0.5 g l^{-1}; potassium dihydrogen phosphate 0.3 g l^{-1}; magnesium sulphate 0.024 g l^{-1}; sodium pyruvate 0.3 g l^{-1}; agar 15.0 g l^{-1}; pH 7.2±0.2). After 3 days of incubation at 28 °C on LB agar, colonies are round, smooth and yellowish. Endospores are formed at the subterminal position of sporangia. The growth conditions are 13–43 °C (optimum 30 °C), pH 5.5–10.0 (optimum pH 9.0) and 0–8% (w/v) (0–1.37 M) NaCl [optimum 0% (w/v) NaCl]. Catalase (EC 1.11.1.6) activity is positive while oxidase (EC 1.1.3.13) activity is weakly positive. In the API 20NE system, positive reactions were obtained for the reduction of nitrate to nitrite, (+)-glucose fermentation and assimilation of (+)-glucose and (+)-maltose, whereas weak gelatin hydrolysis activity of was detected. Negative for nitrite reduction, indole production, aesculin hydrolysis, arginine dihydrolase (EC 3.5.3.6), urease (EC 3.5.1.5), β-galactosidase (EC 3.2.1.23) and assimilation of (+)-arabinose, (+)-mannose, (−)-mannitol, *N*-acetylglucosamine, gluconate, capric acid, adipic acid, malic acid, citrate and phenylacetic acid. In the API ZYM system, positive reactions are obtained for alkaline phosphatase (EC 3.1.3.1), esterase (EC 3.1.1.1) (C4), esterase lipase (EC 3.1.1.1) (C8), leucine arylamidase (EC 3.4.11.1), α-chymotrypsin (EC 3.4.21.1), acid phosphatase (EC 3.1.3.2) and α-glucosidase (EC 3.2.1.20). Valine arylamidase (EC 3.4.11.2), trypsin (EC 3.4.21.4), β-glucuronidase (EC 3.2.1.31) and β-glucosidase (EC3.2.1.21) activities are weakly positive. Negative for lipase (EC 3.1.1.3) (C14), α- and β-galactosidase (EC 3.2.1.22 and EC3.2.1.23), *N*-acetyl-β-glucosaminidase (EC 3.2.1.30), α-mannosidase (EC 3.2.1.24) and α-fucosidase (EC 3.2.1.51). In the API 50 CH system, acid production occurs using (+)-glucose, (−)-fructose, (+)-maltose and (+)-trehalose. But no acid is produced from glycerol, erythritol, (−) and (+)-arabinose, (−)-ribose, (+)- and (−)-xylose, (+)-adonitol, methyl-β-xylopyranoside, (+)-galactose, (+)-mannose, (−)-sorbose, (+)-rhamnose, dulcitol, inositol, (−)-mannitol, (−)-sorbitol, methyl-α-mannopyranoside, methyl-α-glucopyranoside, *N*-acetylglucosamine, amygdalin, arbutin, aesculin ferric citrate, salicin, (+)-cellobiose, (+)-lactose, (+)-melibiose, (+)-sucrose, inulin, (+)-melezitose, (+)-raffinose, starch, glycogen, xylitol, gentiobiose, (+)-turanose, (−)-lyxose, (−)-tagatose, (+)- and (−)-fucose, (+)- and (−)-arabitol, gluconate, potassium 2-ketogluconate and potassium 5-ktogluconate. Can utilize (+)-maltose, (+)-trehalose, α-(+)-glucose, inosine, (+)-lactic acid, acetoacetic acid, acetic acid, glycerol (weakly) and (−)-lactic acid methyl ester (weakly) as sole carbon and energy sources, rather than (+)-cellobiose, gentiobiose, sucrose, (+)-turanose, stachyose, (+)-raffinose, α-(+)-lactose, (+)-melibiose, β-methyl-(+)-glucoside, (−)-salicin, *N*-acetyl-(+)-glucosamine, *N*-acetyl-β-(+)-mannosamine, *N*-acetyl-(+)-galactosamine, *N*-acetyl neuraminic acid, (+)-mannose, (−)-fructose, (+)-galactose, 3-methyl glucose, (+)- and (−)-fucose, (+)-rhamnose, (−)-sorbitol, (−)-mannitol, (+)-arabitol, *myo*-inositol, (+)-glucose-6-phosphate, (−)-fructose-6-phosphate, (−)-aspartic acid, (+)-serine, gelatin, glycyl-(−)-proline, (+)-alanine, (+)-arginine, (+)-aspartic acid, (+)-glutamic acid, (+)-histidine, (+)-pyroglutamic acid, (−)-serine, pectin, (+)-galacturonic acid, (+)-galactonic acid lactone, (+)-gluconic acid, (+)-glucuronic acid, glucuronamide, mucic acid, quinic acid, (+)-saccharic acid, *p*-hydroxyphenylacetic acid, methyl pyruvate, citric acid, α-ketoglutaric acid, (+)- and (−)-malic acid, bromosuccinic acid, tween 40, γ-aminobutryric acid, α-hydroxybutyric acid, β-hydroxy-D,L butyric acid, α-ketobutyric acid, propionic acid and formic acid. Resistant to (µg per disc unless otherwise stated) streptomycin (10), gentamicin (10), kanamycin (30), tobramycin (10), penicillin (10U), ampicillin (10) and amoxicillin/clavulanic acid (20/10) but susceptible to mezlocillin (75), ceftazidime (30), cefatriaxone (30), cefotaxime (30), tetracycline (30), rifampin (5), clindamycin (2), erythromycin (15), chloramphenicol (30) and clarithromycin (15). MK-7 is the predominant isoprenoid quinone. Predominant fatty acids are $C_{15:0}$iso, $C_{16:0}$iso, $C_{16:1}$ω7*c* alcohol, $C_{16:0}$, $C_{17:1}$iso ω10*c* and $C_{17:0}$iso. The major cellular polar lipids are glycolipid, diphosphatidylglycerol, phosphatidylethanolamine and phosphatidylglycerol. The diagnostic cell-wall diamino acid is *meso*-DAP.

The type strain CY-G^T (=MCCC 1K06383^T=KCTC 43348^T) was isolated from a sponge *Diacarnus spinipoculum* from the shallow reef in front of the Interuniversity Institute for Marine Sciences in Eilat, Israel. The genomic DNA G+C content of the type strain is 38.83 mol%. The GenBank accession numbers of the 16S rRNA gene and whole genome sequence of strain CY-G^T are OP869988.1 and CP089997, respectively. The GenBank accession numbers of the COI gene and 28S rRNA gene of sponge *Diacarnus spinipoculum* are OQ384973 and OP895662, respectively.

Funding information
This work was supported by grants from the National Key Research and Development Program of China (grant number 2018YFA0901901).

Acknowledgements
Thanks for Prof. Micha Ilan at Tel-Aviv University for providing the sponge samples.

Author contributions
Z.L., designed the research and project outline. L.G., Q.S. and Y.X., performed microbial isolation. L.G. and J.S., performed polyphasic taxonomy. L.G. performed genome analysis. L.G. and Z.L., drafted and revised the manuscript. All authors read and approved the final manuscript.

Conflicts of interest
The authors declare that they have no conflict of interest.

Ethical statement
This article does not involve any studies with human participants or animals performed by any of the authors.

References

1. Liu Y, Li N, Eom MK, Schumann P, Zhang X, *et al*. *Bacillus ciccensis* sp. nov., isolated from maize (*Zea mays* L.) seeds. *Int J Syst Evol Microbiol* 2017;67:4606–4611.
2. Xu L, Huang X-X, Wang H-T, Tang S-K, Shen B, *et al*. Description and characterization of three endophytic *Bacillaceae* from the halophyte *Suaeda salsa*: *Paenalkalicoccus suaedae* gen. nov., sp. nov., *Cytobacillus suaedae* sp. nov., and *Bacillus suaedae* sp. nov. *Int J Syst Evol Microbiol* 2022;72:005337.
3. Zhang J, Wang J, Fang C, Song F, Xin Y, *et al*. *Bacillus oceanisediminis* sp. nov., isolated from marine sediment. *Int J Syst Evol Microbiol* 2010;60:2924–2929.
4. Wei X, Xin D, Xin Y, Zhang H, Wang T, *et al*. *Bacillus depressus* sp. nov., isolated from soil of a sunflower field. *Antonie van Leeuwenhoek* 2016;109:13–20.
5. Liu B, Liu G-H, Sengonca C, Schumann P, Ge C-B, *et al*. *Bacillus solani* sp. nov., isolated from rhizosphere soil of a potato field. *Int J Syst Evol Microbiol* 2015;65:4066–4071.
6. Liu B, Liu G-H, Sengonca C, Schumann P, Wang J-P, *et al*. *Bacillus praedii* sp. nov., isolated from purplish paddy soil. *Int J Syst Evol Microbiol* 2017;67:2823–2828.
7. Shi R, Yin M, Tang S-K, Lee J-C, Park D-J, *et al*. *Bacillus luteolus* sp. nov., a halotolerant bacterium isolated from a salt field. *Int J Syst Evol Microbiol* 2011;61:1344–1349.
8. Hong SW, Park JM, Kim SJ, Chung KS. *Bacillus eiseniae* sp. nov., a swarming, moderately halotolerant bacterium isolated from the intestinal tract of an earthworm (*Eisenia fetida* L.). *Int J Syst Evol Microbiol* 2012;62:2077–2083.
9. Lin S-Y, Hameed A, Liu Y-C, Hsu Y-H, Lai W-A, *et al*. *Bacillus formosensis* sp. nov., isolated from pesticide wastewater. *Int J Syst Evol Microbiol* 2015;65:3800–3805.
10. Ivone VM, Vania F, AnaRL, Alexandre Ldc, Cathrin S, *et al*. *Bacillus purgationiresistans* sp. nov., isolated from a drinking-water treatment plant. *Int J Syst Evol Microbiol* 2012;62:71–77.
11. Seiler H, Wenning M, Schmidt V, Scherer S. *Bacillus gottheilii* sp. nov., isolated from a pharmaceutical manufacturing site. *Int J Syst Evol Microbiol* 2013;63:867–872.
12. Vaishampayan P, Probst A, Krishnamurthi S, Ghosh S, Osman S, *et al*. *Bacillus horneckiae* sp. nov., isolated from a spacecraft-assembly clean room. *Int J Syst Evol Microbiol* 2010;60:1031–1037.
13. Seiler H, Schmidt V, Wenning M, Scherer S. *Bacillus kochii* sp. nov., isolated from foods and a pharmaceuticals manufacturing site. *Int J Syst Evol Microbiol* 2012;62:1092–1097.
14. Chen Y, Sang J, Sun W, Song Q, Li Z. *Mycetocola spongiae* sp. nov., isolated from deep-sea sponge *Cacospongia mycofijiensis*. *Int J Syst Evol Microbiol* 2022;72:005291.
15. Ardui S, Ameur A, Vermeesch JR, Hestand MS. Single molecule real-time (SMRT) sequencing comes of age: applications and utilities for medical diagnostics. *Nucleic Acids Res* 2018;46:2159–2168.
16. Lagesen K, Hallin P, Rødland EA, Staerfeldt H-H, Rognes T, *et al*. RNAmmer: consistent and rapid annotation of ribosomal RNA genes. *Nucleic Acids Res* 2007;35:3100–3108.
17. Boden R, Hutt LP, Rae AW. Reclassification of *Thiobacillus aquaesulis* (Wood & Kelly, 1995) as *Annwoodia aquaesulis* gen. nov., comb. nov., transfer of *Thiobacillus* (Beijerinck, 1904) from the *Hydrogenophilales* to the *Nitrosomonadales*, proposal of *Hydrogenophilalia* class. nov. within the '*Proteobacteria*', and four new families within the orders *Nitrosomonadales* and *Rhodocyclales*. *Int J Syst Evol Microbiol* 2017;67:1191–1205.
18. Saitou N, Nei M. The neighbor-joining method: a new method for reconstructing phylogenetic trees. *Mol Biol Evol* 1987;4:406–425.
19. Felsenstein J. Evolutionary trees from DNA sequences: a maximum likelihood approach. *J Mol Evol* 1981;17:368–376.
20. Rzhetsky A, Nei M. A simple method for estimating and testing minimum evolution trees. *Mol Biol Evol* 1992;9:945–967.
21. Tamura K, Stecher G, Kumar S. MEGA11: molecular evolutionary genetics analysis version 11. *Mol Biol Evol* 2021;38:3022–3027.
22. Jain C, Rodriguez-R LM, Phillippy AM, Konstantinidis KT, Aluru S. High throughput ANI analysis of 90K prokaryotic genomes reveals clear species boundaries. *Nat Commun* 2018;9:5114.
23. Varghese NJ, Mukherjee S, Ivanova N, Konstantinidis KT, Mavrommatis K, *et al*. Microbial species delineation using whole genome sequences. *Nucleic Acids Res* 2015;43:6761–6771.
24. Meier-Kolthoff JP, Auch AF, Klenk HP, Göker M. Genome sequence-based species delimitation with confidence intervals and improved distance functions. *BMC Bioinformatics* 2013;14:60.
25. Wayne LG, Brenner DJ, Colwell RR, Grimont PAD, Kandler O, *et al*. Report of the ad hoc committee on reconciliation of approaches to bacterial systematics. *Int J Syst Evol Microbiol* 1987;37:463–464.
26. Blin K, Shaw S, Kloosterman AM, Charlop-Powers Z, van Wezel GP, *et al*. antiSMASH 6.0: improving cluster detection and comparison capabilities. *Nucleic Acids Res* 2021;49:W29–W35.
27. Chen Y-G, Cui X-L, Pukall R, Li H-M, Yang Y-L, *et al*. *Salinicoccus kunmingensis* sp. nov., a moderately halophilic bacterium isolated from a salt mine in Yunnan, south-west China. *Int J Syst Evol Microbiol* 2007;57:2327–2332.

28. Sasser M. Technical note 101: identification of bacteria by gas chromatography of cellular fatty acids. *Newark: MIDI, Inc North* 1990;20:1–7.
29. Collins MD. Isoprenoid quinone analyses in bacterial classification and identification. *Soc Appl Bacteriol Tech Ser* 1985;20:267–287.
30. Minnikin DE, O'Donnell AG, Goodfellow M, Alderson G, Athalye M, *et al*. An integrated procedure for the extraction of bacterial isoprenoid quinones and polar lipids. *J Microbiol Meth* 1984;2:233–241.
31. Tindall BJ. Lipid composition of *Halobacterium lacusprofundi*. *FEMS Microbiol Lett* 1990;66:199–202.
32. Komagata K, Suzuki K. Lipid and cell-wall analysis in bacterial systematics. *Methods Microbiol* 1987;19:161–207.
33. Goodfellow M, Orchard VA. Antibiotic sensitivity of some nocardioform bacteria and its value as a criterion for taxonomy. *J Gen Microbiol* 1974;83:375–387.